

---

# NONTHERMAL RADIATION OF THE CRAB NEBULA

---

F.A. Aharonian

*Max Planck Institut für Kernphysik, Postfach 103980,  
D-69029 Heidelberg, Germany, aharon@fel.mpi-hd.mpg.de*

A.M. Atoyan

*Yerevan Physics Institute, Armenia, atoyan@boris.mpi-hd.mpg.de*

---

## Abstract

The radiation mechanisms contributing to formation of the nonthermal spectrum of the Crab Nebula, as well as the information that could be derived from future observations in different energy bands, are discussed.

## 1. Introduction

The Crab Nebula is a unique cosmic laboratory with an unprecedentedly broad spectrum of the observed nonthermal radiation which extends throughout 21 (!) decades of frequencies – from radio wavelengths to very high energy  $\gamma$ -rays (see Fig. 1). This emission is dominated by two major mechanisms connected with interactions of relativistic electrons with the nebular magnetic and photon fields. While the synchrotron component is responsible for the radiation from radio to relatively low energy  $\gamma$ -rays ( $E < 1$  GeV), the inverse Compton (IC) scattering of electrons is thought as the most probable mechanism for very high energy  $\gamma$ -rays discovered in the late 80's by the Whipple collaboration (Weekes et al. 1989).

The typical energies of electrons responsible for production of synchrotron photons in different energy bands of the Crab spectrum are indicated in Fig. 1. Note that although the conclusion about highest energy electrons is still based on a model (although well justified) assumption about the synchrotron origin of the hard X-rays/low-energy  $\gamma$ -rays, the detection of  $\gamma$ -rays well above  $10^{13}$  eV is an *unambiguous* evidence of effective acceleration of particles beyond  $10^{14}$  eV.

It is commonly accepted that the synchrotron nebula is powered by the relativistic wind of electrons generated at the pulsar and terminated by a standing reverse shock wave at a distance  $r_s \sim 0.1$  pc (Rees and Gun 1974). The relativistic MHD models, even in their simplified form (e.g. ignoring the axisymmetric structure of the wind and its interaction with the optical filaments), successfully describe the general characteristics of the synchrotron nebula, and predict realistic distributions of relativistic electrons and magnetic field in the downstream region behind the shock (e.g. Kennel and Coroniti 1984, hereafter KC84).

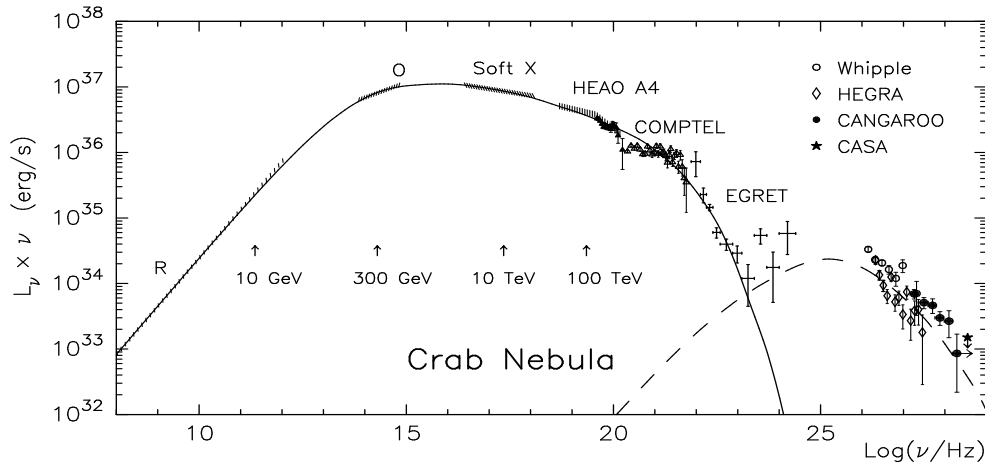


Fig. 1. Nonthermal radiation of the Crab Nebula. In the  $\gamma$ -ray domain only the recently reported fluxes are shown: COMPTEL (van der Meulen et al. 1998), EGRET (Fierro 1996), Whipple (Mohanty et al. 1998), HEGRA (Aharonian et al. 1997), CANGAROO (Tanimori et al. 1998), CASA (Borione et al. 1997). The solid and dashed curves correspond to the synchrotron and inverse Compton components of radiation, respectively, calculated in the framework of the spherically symmetric MHD wind model of KC84.

While the synchrotron and IC mechanisms seem to provide a reasonable explanation of the overall nonthermal radiation of the Crab Nebula (see Fig. 1), one cannot exclude possible deviations in different frequency domains from the simplified picture of the outer nebula described by the spherically symmetric MHD models. Indeed, the recent imaging of the Crab Nebula by the Hubble Space Telescope and ROSAT revealed a very complex structure of the inner part of the nebula consisting of features like wisps, jets, knots, *etc.* (Hester et al. 1995). This shows that we are far from complete understanding of the physics of interaction of the pulsar wind with the synchrotron nebula, and ensures that this object remains a great challenge for future theoretical work. Although it seems unlikely that the incorporation of the hot spots would dramatically change the overall nonthermal spectrum of the Crab Nebula, nevertheless they could introduce non-negligible spectral features in the X-ray and  $\gamma$ -ray domains. Furthermore, a significant production of high-energy  $\gamma$ -rays, on top of the IC radiation originating in the synchrotron nebula, could occur in the filaments, provided that the relativistic particles were partially confined in these high density regions. Within this scenario, both the bremsstrahlung of relativistic electrons, and  $\pi^0$ -decay  $\gamma$ -rays produced by protons might significantly affect the overall  $\gamma$ -ray spectrum.

## 2. Synchrotron and IC radiation of the Crab Nebula

To calculate the nonthermal radiation of the Crab Nebula, one has to specify the spatial distribution of the magnetic field, the acceleration site(s) and the injection spectrum of the relativistic electrons, as well as the character of their propagation in the nebula. Remarkably, the MHD model of KC84 provides all these parameters, in particular allows self-consistent calculation of the spatial and spectral distribution of high energy electrons, freshly accelerated at the wind termination shock and injected

into the nebula (*wind* electrons). Arons and co-workers (see e.g. Arons 1996) have shown that the wind termination shock is able to accelerate particles up to  $\sim 10^{15}$  eV.

Meanwhile the radio emission of the nebula requires an additional low energy ( $E \leq 200$  GeV) component of electrons (*radio* electrons) accumulated, most probably, during the whole history of the Crab (KC84). Although the origin and site(s) of this “relic” component are not yet established, it can be easily incorporated into the calculations of the broad-band synchrotron spectrum with a minimum number of assumptions based on radio observations (Atoyan and Aharonian 1996, hereafter AA96).

Fig. 1 demonstrates good agreement of calculations with the observed spectrum of the Crab Nebula up to hard X-rays, and a reasonable explanation of the  $\gamma$ -ray fluxes up to 1 GeV by the synchrotron radiation. The best fit is reached by the following combination of the spectra of the *radio* and *wind* electrons: (1)  $n_{\text{re}}(E) \propto E^{-\alpha_{\text{re}}} \exp(-E/E_c)$  with  $\alpha_{\text{re}} = 1.52$  and  $E_c = 150$  GeV, and (2)  $n_{\text{we}}(E) \propto (E_* + E)^{-\alpha_{\text{we}}} \exp(-E/E_1)$  with  $\alpha_{\text{we}} = 2.4$ ,  $E_* = 200$  GeV, and  $E_1 = 2.5 \cdot 10^{15}$  eV. The presentation of the spectrum of the *wind* electrons  $n_{\text{we}}(E)$  in such form provides a necessary (and natural in the framework of MHD model) flattening of the spectrum below  $E_* \sim 200$  GeV. The transition from the hard to steep power-laws in the total (*radio* + *wind*) electron spectrum at energies around 100 GeV accounts for the sharp steepening of the spectrum at IR/optical wavelengths. Therefore detailed spectroscopic measurements in this energy region would allow us to specify more precisely the values of  $E_c$  and  $E_*$  which define the degree of “smoothness” of transition from *radio* to *wind* electrons. An independent information about the electrons in this transition region is contained in the 10 to 100 GeV  $\gamma$ -rays produced by the same electrons upscattering the ambient low-frequency radiation. Meanwhile, determination of the high energy cutoff  $E_1$  in  $n_{\text{we}}(E)$  is contingent of spectroscopic measurements of  $\gamma$ -rays in the 1 MeV to 1 GeV energy band.

The existence of ultra-relativistic electrons in the synchrotron nebula provides production of detectable TeV  $\gamma$ -ray fluxes through the IC scattering (Gould 1965). Since the target radiation fields which play major role in the production of IC  $\gamma$ -rays of the Crab Nebula (synchrotron, thermal far IR, and 2.7 K background radiations) are well known, the flux of IC  $\gamma$ -rays can be calculated with good accuracy. For the given flux of synchrotron X-rays, the number of TeV electrons strongly depends on the nebular magnetic field. Therefore the IC  $\gamma$ -ray fluxes are very sensitive to the average magnetic field:  $I(\geq 1 \text{ TeV}) \simeq 8 \cdot 10^{-12} (\bar{B}/0.3 \text{ mG})^{-2.1} \text{ ph/cm}^2\text{s}$ . Thus the comparison of the predicted and observed TeV  $\gamma$ -ray fluxes allows determination of the magnetic field in the central  $r \sim 0.5$  pc region (where the bulk of X-rays and TeV  $\gamma$ -rays are produced) with accuracy  $\Delta B/\bar{B} \simeq 0.5(\Delta I/I)$ . Although the statistical significance of  $\gamma$ -ray observations of the Crab Nebula is very high, the systematic uncertainties in the flux estimates remain rather large,  $\Delta I/I \sim 1$  (see Fig.1). Even with present uncertainties, the TeV observations favor the magnetic field in the X-ray production region within  $\bar{B} \sim 0.2 - 0.3$  mG, which is in agreement with the estimated equipartition field (Marsden et al. 1984).

The shape of the spectrum of IC  $\gamma$ -rays is rather stable to the basic parameters of the nebula (AA96), in particular, it is almost independent of the parameter  $\sigma$  (the ratio of the electromagnetic energy flux to the particle energy flux at the shock) which in the framework of MHD model defines the spatial distribution of the magnetic field  $B(r)$  at  $r \geq r_s$ . Although the calculations in Fig. 1 correspond to  $\sigma = 0.005$ , the

measured synchrotron fluxes can be equally well fitted by the  $\sigma$  between 0.001 and 0.01. Indeed, since at distances  $\geq 3r_s$ , where the bulk of synchrotron and IC photons are produced, the magnetic field  $B(r)$  depends rather weakly on  $\sigma$  (see KC84), only minor changes in the assumed injection spectrum of electrons are required to provide the same synchrotron spectrum for different  $\sigma$  within 0.001-0.01. Consequently, as far as the target photon fields for IC  $\gamma$ -rays are fixed, there is no room for strong dependence of the calculated IC fluxes on  $\sigma$ .

This conclusion opposes to the statement of De Jager and Harding (1992) and De Jager et al (1996; hereafter DJ96) about significant dependence of IC  $\gamma$ -ray fluxes on  $\sigma$ . The method of calculations of IC radiation used in these papers is based on the extraction of the “prompt” spectrum of electrons in the nebula,  $N_e(E, r)$ , using the spatial and energy distribution of the synchrotron radiation  $F(\nu, r)$ , with an additional assumption about the structure of magnetic field  $B(r)$  taken from KC84. Although quite appropriate in principle, this method seems to be not well justified, at least presently, taken the fact of the lack of proper information on  $F(\nu, r)$ , especially at X-rays – the counterparts of TeV  $\gamma$ -rays. Such uncertainties leave large room for ambiguities in the  $N_e(E, r)$ , and consequently in the IC  $\gamma$ -ray spectra. Therefore it is crucial to control the accuracy of the procedure by comparison of the calculated synchrotron spectra (based on the *approximately* reconstructed  $N_e(E, r)$ ) with the observed ones. Since such comparison is missing in the above mentioned papers, we can only guess that the claimed strong  $\sigma$ -dependence of the TeV fluxes does not exceed the accuracy of calculations. In this context, it is worth noticing that in DJ96, where the authors suggested an interesting idea of the synchrotron radiation due to the *second* population of highest energy electrons (see below), they show (Figure 1 in DJ96) the IC spectra calculated for different  $\sigma$  without presentation of the relevant synchrotron spectra of the *main* electron component. On the other hand in the same Figure 1 of DJ96 is shown the hard synchrotron spectrum (“MeV bump”) produced by the second population of electrons, but without indication of contribution of the latter to the IC  $\gamma$ -ray fluxes.

In Fig. 1 we show the combined synchrotron and IC components of radiation, calculated in the framework of spherically symmetric MHD model, which describe fairly well the flux levels of the Crab Nebula over the whole range of observed frequencies. Meanwhile the “zoom” of Fig. 1 reveals some peculiarities in the spectrum, in particular at 1-10 MeV, 1-10 GeV, and perhaps also at  $\geq 10$  TeV energies which could not be easily interpreted within the simplified synchrotron-Compton model. Below we discuss possible ways to account for these features.

### 3. Second High Energy Synchrotron Component

The recent spectral measurements of the unpulsed radiation of the Crab by COMPTEL revealed an unexpected flattening of the spectrum at energies 1-10 MeV (van der Meulen et al. 1998) which follows after well established steepening of the spectrum above 100 keV (Jung 1989, Bartlett et al. 1996). Since such sharp feature hardly could be attributed to peculiarities in the injection spectrum of shock accelerated electrons, more natural interpretation of this spectral feature could be given assuming the existence of an additional radiation component. Explanation of this radiation excess in terms of nuclear  $\gamma$ -ray line emission is not supported by observations (van der Meulen

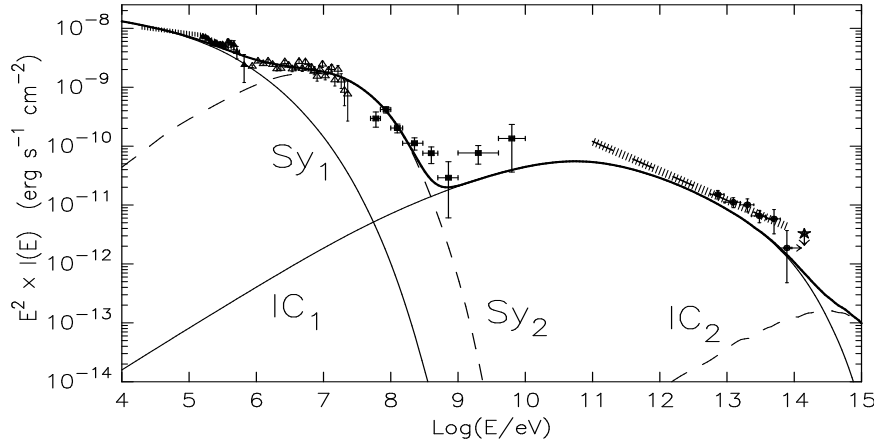


Fig. 2. Synchrotron and IC radiation components produced by the first (solid) and second (dashed) populations of electrons (see text). The heavy solid line shows the total flux. The hatched region corresponds to  $I(E) = (2.5 \pm 0.4) (E/1 \text{ TeV})^{-2.5} \text{ cm}^{-2} \text{ s}^{-1} \text{ TeV}^{-1}$  which generally describes the flux levels from 300 GeV to 70 TeV reported by different groups.

et al. 1998), and more importantly, it contradicts to the total luminosity of the Crab Nebula since only  $\xi \leq 10^{-4}$  part of the energy losses of nonrelativistic protons and nuclei is released in prompt  $\gamma$ -ray lines, while its main part goes to heating of the ambient gas, and thus should be shown up in the form of thermal radiation with unacceptably high luminosity  $L_{\text{thermal}} \sim \xi^{-1} L_{\text{obs}}(1 - 10 \text{ MeV}) \geq 10^{40} \text{ erg/s}$ .

While remaining in the framework of the hypothesis of the synchrotron origin of the radiation up to 1 GeV, the steepening above 100 keV implies an exponential cutoff in the injection spectrum of the *wind* electrons at energies smaller than  $E_1 = 2.5 \cdot 10^{15} \text{ eV}$  used in Fig. 1. If so, the flat spectrum observed by COMPTEL requires the second population of high energy electrons (DJ96). In Fig. 2 we present a possible fit of the observed fluxes up to 1 GeV by two-component synchrotron emission. The first component is attributed to the same *wind* electrons as in Fig. 1 but with  $E_1 = 5 \cdot 10^{14} \text{ eV}$ . For the second component we have to suppose very hard acceleration spectrum, for example of Maxwellian type,  $n_2(E) \propto E^2 \exp(-E/E_2)$  with  $E_2 = 5.5 \cdot 10^{14} \text{ eV}$ . Although here  $E_1 \approx E_2$ , actually the mean energy of the second population  $\bar{E} = 3E_2 \simeq 1.6 \cdot 10^{15} \text{ eV}$  is larger than the highest energy particles  $E \sim E_1$  effectively present in the first population. Note that the needed acceleration power in the second electron population is only  $P_2 \sim L_{\text{obs}}(1 - 10 \text{ MeV}) \sim 10^{36} \text{ erg/s}$ , i.e. less than 1% of the first (*main*) population,  $P_1 \sim 3 \cdot 10^{38} \text{ erg/s}$ . This explains the small contribution of the second electron population into the total IC  $\gamma$ -ray fluxes up to energies  $10^{14} \text{ eV}$  (see Fig. 2).

The possible sites of acceleration of the second electron population could be the peculiar compact regions such as wisps, knots, etc. Since the equipartition magnetic field in these regions is estimated as high as few mG (in that case  $E_2$  is reduced to  $\simeq 10^{14} \text{ eV}$ ) the highest energy electrons could not escape the acceleration sites due to severe synchrotron losses. Although these highly variable structures with typical size  $0.2''$  (Hester 1995) are not resolvable by low-energy  $\gamma$ -ray detectors, the confirmation of variability of 1-150 MeV emission reported in DJ96 would be a direct proof for the synchrotron origin of the “MeV bump”.

#### 4. Bremsstrahlung and $\pi^0$ -decay Gamma Rays ?

The second feature seen in Fig. 1 and Fig. 2 is the deficit in the predicted IC fluxes compared to the reported fluxes at GeV energies<sup>1</sup>. Indeed, the expected IC  $\gamma$ -ray flux in this energy region is estimated within 20% accuracy as  $I(1 - 10 \text{ GeV}) \simeq 10^{-8} (\bar{B}/0.3 \text{ mG})^{-1.3} \text{ ph/cm}^2\text{s}$  (AA96). For the equipartition magnetic field  $B \simeq 0.3 \text{ mG}$  this flux is by a factor of 5 below of the one measured by EGRET. In order to explain the measured fluxes in this energy region, an additional component of GeV radiation was suggested in DJ96, which the authors in their best-fit “synchrotron+IC” model call as a *second IC power-law component*. Meanwhile, to increase the IC flux one has to suppose for the magnetic field in the radio nebula (where the low energy  $\gamma$ -rays are produced)  $B \sim 10^{-4} \text{ G}$ . However, this is a rather uncomfortable value since it would imply the energy in radio electrons  $W_e \simeq 7 \cdot 10^{48} \text{ erg}$ , while the energy in the magnetic field were by a factor of 30 smaller, which makes rather problematic the confinement of electrons in the nebula. Thus, if the high EGRET flux above 1 GeV really originates in the nebula, then invocation of other mechanism(s) for additional production of  $\gamma$ -rays, e.g. due to interactions of relativistic particles with the ambient nebular gas (AA96), seems unavoidable.

**Bremsstrahlung gamma-rays.** For the mean gas density in the nebula  $\bar{n} \approx 5 \text{ cm}^{-3}$ , the flux of the bremsstrahlung  $\gamma$ -rays cannot exceed 15% of the flux of IC  $\gamma$ -rays. In fact, in the Crab Nebula the gas is concentrated mainly in dense filaments where  $n \sim 10^3 \text{ cm}^{-3}$  (Davidson and Fesen 1985). In the case of uniform distribution of relativistic electrons throughout the nebula the *effective* gas density is defined by the mean density of the nebula,  $n_{\text{eff}} \approx \bar{n}$ . However, if electrons are trapped, at least partially, in the regions of high density, i.e. if they propagate inside the filaments *slower* than outside, then  $n_{\text{eff}} \gg \bar{n}$  (for details see AA96). The fluxes of bremsstrahlung  $\gamma$ -rays calculated for  $n_{\text{eff}} = 50 \text{ cm}^{-3}$  are shown in Fig. 3. The contribution of the “amplified” bremsstrahlung flux not only could explain the measured GeV  $\gamma$ -ray fluxes, but also would significantly modify the spectrum at very high energies. Indeed, in the energy range between 100 GeV and 10 TeV the superposition of the IC and the “amplified” bremsstrahlung components results in almost power-law spectrum with an index  $\alpha_\gamma \simeq (2.5 - 2.7)$  in contrast to the curved IC  $\gamma$ -ray spectrum *alone*, which is hard at  $E \simeq 100 \text{ GeV}$  ( $\alpha_\gamma \simeq 2.0$ ), but becomes significantly steeper at higher energies ( $\alpha_\gamma \simeq 2.7$  at  $E \simeq 10 \text{ TeV}$ ).

**$\pi^0$ -decay gamma-rays.** Interactions of the nucleonic component of accelerated particles (which may in principle acquire significant part of the power of relativistic wind at the reverse shock; see Arons 1996), with the ambient gas lead to production of  $\gamma$ -rays through secondary  $\pi^0$ -decays. However, since the average gas density in the nebula is low, the contribution of this mechanism to the  $\gamma$ -radiation could be detectable only in the case of partial confinement of relativistic particles in the filaments, so that  $n_{\text{eff}} \gg \bar{n}$ . If so, the  $\pi^0$ -decay  $\gamma$  rays may effectively show up (on top of the steep IC spectrum) at multi-TeV energies (AA96). From this point of view, the recently reported detection of

---

1 In Figs. 2,3 we show the spectral points reported by Nolan et al. (1993) which are somewhat different from the results of the latest analysis (Fierro 1996) shown in Fig. 1. The irregularities in the 1-10 GeV region could be due to the deficit of sufficient photon statistics in smaller energy bins used in the analysis of Fierro (1996).

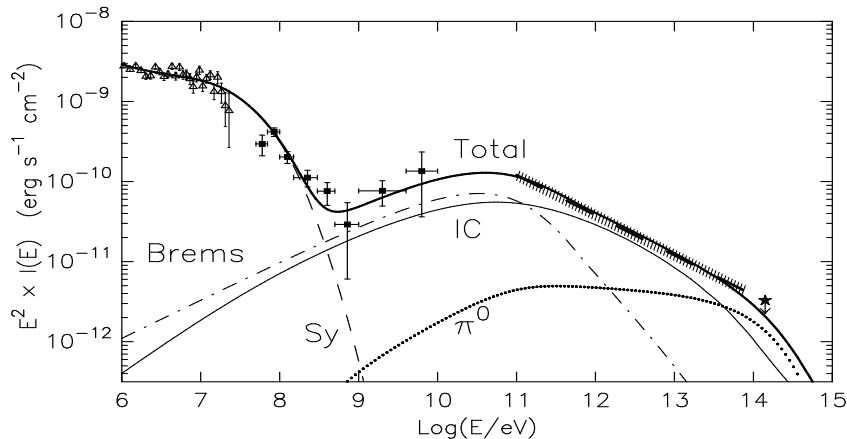


Fig. 3. The contributions of different  $\gamma$ -ray production mechanisms to the total nonthermal radiation of the Crab Nebula. The Synchrotron and IC components are the same as in Fig.2. The bremsstrahlung and  $\pi^0$ -decay  $\gamma$ -ray fluxes are calculated for  $n_{\text{eff}} = 50 \text{ cm}^{-3}$  (see text).

up to 70 TeV  $\gamma$ -radiation from the Crab by the CANGAROO collaboration (Tanimori et al. 1998) may have significant implications concerning the content of the wind and propagation/interaction of accelerated particles in the filaments. Although the CANGAROO fluxes do not contradict, within the uncertainties in the nebular magnetic field, to the IC origin of the radiation, the reported differential power-law spectrum from several TeV to 50 TeV with an index  $\alpha_\gamma = 2.53 \pm 0.18$  seems to be essentially harder than the predicted IC spectrum ( $\alpha_\gamma \simeq 3$  at 30 TeV).

In Fig. 3 we show the spectrum of  $\pi^0$ -decay  $\gamma$ -rays calculated for the power-law differential spectrum of accelerated protons with  $\alpha_p = 2.1$ , exponential cutoff at  $E = 10^{15}$  eV and significant flattening below  $E \sim 1$  TeV, as it is expected from the wind acceleration models. For  $n_{\text{eff}} = 50 \text{ cm}^{-3}$  used in Fig. 3, the shown  $\pi^0$ -decay fluxes correspond to total energy in accelerated protons  $W_p = 1.5 \cdot 10^{48}$  erg, a quite acceptable amount from the point of view of the energy budget of the Crab. It is interesting to note that for the chosen parameters the superposition of 3 components of radiation – “IC+bremsstrahlung+ $\pi^0$ ” – results in the power-law spectrum with  $\alpha_\gamma \simeq 2.5$  over the entire energy range from 100 GeV to 100 TeV. This spectrum significantly differs from the pure IC spectrum, and provides a better fit to the reported data the compilation of which is presented in Fig. 2 and 3 by the hatched zone. However, given the large uncertainties in the reported  $\gamma$ -ray fluxes, presently we could not make a strong statement about the existence of the bremsstrahlung and  $\pi^0$  signatures in the Crab spectrum.

## 5. Discussion

The Crab Nebula, one of the most comprehensively studied objects on the sky, is detectable from 10 MHz radio waves to multi-TeV  $\gamma$ -rays. The multiwavelength observations of the Crab Nebula have already provided deep insight into the origin of the source dominated by nonthermal energy in the form of magnetic fields and relativistic electrons. Meanwhile many details remain still unresolved, and should be addressed by

future observations. Importantly, the fluxes of the source exceed, by at least one order of magnitude, the sensitivities of the current or planned instruments at practically all frequencies of the observed spectrum. This ensures further significant progress in understanding of complex processes of interaction of the relativistic pulsar wind with the nebula. Below we briefly outline some problems which could be answered, hopefully in the near future, by new observations in different energy bands.

**Probing the magnetic field and electrons in the synchrotron nebula.** The most informative frequency band to probe the acceleration site(s) and the character of propagation of the *wind electrons* in the nebula is the X-ray domain. The AXAF, with its subarcsecond imaging capability and excellent spectral resolution (Elvis 1997), seems to be an ideal instrument for such study. Meanwhile the synchrotron data alone, strictly speaking, tell us only about the product of the energy densities of the magnetic field and relativistic electrons. These parameters could be disentangled using additional information contained in the IC  $\gamma$ -rays produced by the same electrons. Although the limited angular resolution of  $\gamma$ -ray detectors does not allow, at least presently, mapping of the source on subarcmin scales, the measurements of integral fluxes of IC  $\gamma$ -rays at different energies, being coupled with synchrotron radiation in relevant energy bands, could compensate this disadvantage.

Indeed, since the TeV  $\gamma$ -rays are produced by IC scattering of electrons responsible for the observed keV X-rays, the estimate of the magnetic field based on keV/TeV data relates to the central  $r \sim 0.5$  pc region of the Crab Nebula. The model-independent estimate of the magnetic field in the outer parts of the (optical) nebula can be provided by measurements of  $\gamma$ -ray fluxes at  $E \sim 100$  GeV. Similarly, the fluxes of  $E \geq 10$  TeV  $\gamma$ -rays, combined with hard X-ray data ( $E \geq 100$  keV), could allow determination of the magnetic field in the vicinity of the wind shock front at  $r \sim 0.1$  pc. Remarkably, as far as the target photon fields for IC  $\gamma$ -rays are well known, the accuracy of the estimate of the magnetic field could be better than 25%, provided that the  $\gamma$ -ray fluxes are measured with accuracy better than 50%. Despite the current large uncertainties in the reported TeV  $\gamma$ -ray fluxes, caused essentially by the uncertainties in the absolute calibration of the telescopes, it is believed that such accuracy will be reached soon by imaging Cherenkov telescopes like Whipple, HEGRA, and CAT <sup>2</sup>.

The detection of the Crab well beyond 10 TeV by the CANGAROO group is very encouraging, but it would be very important to have independent measurements in this energy region. Also, it is expected that in 1 or 2 years the  $\gamma$ -ray flux measurements from the Crab will be extended down to 30 GeV by low-energy threshold atmospheric Cherenkov detectors like STACEE and CELEST. Besides of the determination of the magnetic field in the optical nebula, good spectroscopy at these energies could provide important information about the spectrum of electrons in the transition region from the *radio* electrons to *wind* electrons.

While at energies between 1 and 10 TeV the IC scattering dominates over all other possible radiation mechanisms, at energies below 1 TeV and above 10 TeV other processes connected with interaction of the relativistic particles with the nebular gas might contribute to the production of  $\gamma$ -rays as much as the IC does. Therefore deter-

---

<sup>2</sup> for description of current and planned ground-based  $\gamma$ -ray detectors mentioned in this paper see e.g. the recent reviews by Aharonian and Akerlof (1997) and Fegan(1997).



mination of the magnetic field based on  $\gamma$ -ray fluxes in these energy regions requires separation of the IC contribution from the possible contamination due to  $\gamma$ -rays of other origin. The shape of the spectrum of IC  $\gamma$ -rays is rather stable to the basic parameters of the nebula. While at GeV energies the IC spectrum is very hard, with power-law index  $\alpha_\gamma \approx 1.5$ , in the VHE region the spectrum gradually steepens from  $\alpha_\gamma \approx 2$  at  $E \sim 100$  GeV to  $\alpha_\gamma \approx 2.5$  at  $E \sim 1$  TeV, and  $\alpha_\gamma \approx 2.7$  at  $E \sim 10$  TeV (see Fig. 1). Confirmation of this spectral shape seems one of the important issues to be addressed by new observations, in particular by the stereoscopic systems of imaging atmospheric Cherenkov telescopes which provide good spectrometry with energy resolution  $\leq 20\%$ , and high precision of localization of the point VHE sources with subarcmin accuracy (Aharonian and Akerlof 1997). Although this still is not sufficient for adequate study of the angular structure of the VHE  $\gamma$ -ray production region in the Crab, in combination with expected large photon statistics it could give an answer whether the observed  $\gamma$ -rays are produced in the *nebula*, or should they be attributed to the unpulsed radiation of the pulsar (Cheung and Cheng 1994, Bogovalov and Kotov 1995, Stepanian 1995).

**Interaction of accelerated particles with filaments.** Although the uncertainties in the reported fluxes at energies 1-10 GeV do not allow one to claim about the strong conflict between the observations and the predicted IC  $\gamma$ -ray fluxes, the confirmation of high EGRET fluxes by future observations, e.g. by the GLAST (Bloom 1996), would require more effective mechanism(s) responsible for  $\gamma$ -ray production in this energy region. The bremsstrahlung of *radio* electrons seems to be an intriguing possibility. In particular, it implies an effective confinement of the relativistic particles in dense filaments to provide sufficiently high *effective* gas density (“seen” by relativistic particles)  $n_{\text{eff}} \geq 50 \text{ cm}^{-3}$ . In its turn, this implies essentially different speed and character of propagation of relativistic particles in the filaments and in the rest of the nebula.

The enhanced rate of interactions of relativistic particles with the gas due to their confinement in high density regions, opens possibility to probe the content of the pulsar wind by searching for  $\pi^0$   $\gamma$ -rays in the spectrum of the Crab at very high energies. Indeed, for the *effective* gas density  $n_{\text{eff}} \geq 50 \text{ cm}^{-3}$ , the total energy of accelerated protons (nuclei)  $W_p \leq 2 \cdot 10^{48}$  erg, quite reasonable amount for the energy budget of the Crab, would be sufficient for significant modification (hardening) of the resulting “IC+ $\pi^0$ ” spectrum. If confirmed by future accurate spectroscopic measurements, the relatively hard spectrum of  $\gamma$ -rays above 10 TeV reported by CANGAROO ( $\alpha_\gamma \leq 2.7$ ), will indicate the acceleration of nucleonic component in the Crab up to energies  $10^{15}$  eV, as well as high concentration of relativistic particles in dense gas regions. Interestingly, since this will unavoidably result in the enhanced bremsstrahlung  $\gamma$ -rays as well, the total “IC+bremsstrahlung+ $\pi^0$ ” radiation spectrum is expected to be of almost single power-law form above 100 GeV over three decades in energy.

**Origin of hard (MeV) synchrotron radiation.** The apparent steepening in the synchrotron spectrum above 100 keV followed by hard MeV radiation (“MeV bump”) can be naturally interpreted as superposition of two different radiation components, both, most probably, of the synchrotron origin. If the first component is attributed to the diffuse emission of the synchrotron nebula, the second component could originate in one or few compact structures, e.g. wisps or knots, where the strong magnetic field ( $B \geq 10^{-3}$  G) could create favorable conditions for both effective acceleration of high-

est energy electrons and production of synchrotron radiation up to several 100 MeV. The limited angular resolution of hard X-ray/soft  $\gamma$ -ray detectors does not allow direct identification of these compact structures. On the other hand, since the cooling time of electrons producing MeV synchrotron radiation does not exceed the light crossing time of these compact structures, the detailed study of the spectrum and flux variability of radiation in this energy domain by future INTEGRAL (Winkler 1996) and GLAST (Bloom 1996) missions, could compensate, to some extent, the lack of spatial information.

Meanwhile, direct information about the site(s) of the synchrotron “MeV bump” could be obtained in soft X-rays by AXAF. Indeed, even in the case of extremely hard spectrum (e.g. monoenergetic or Maxwellian type) of electrons responsible for the “MeV bump”, the energy flux of this component at 1-10 keV range cannot be less than  $10^{-11}$  erg/cm<sup>2</sup>s, so it should be easily detected by AXAF even if this flux is due to superposition of large number of subarcsecond structures. However, detection of these structures in X-rays will be not yet enough to identify them as the sites of “MeV bump”. The important criteria for such identification is the expected very hard spectrum at keV energies, namely, essentially harder than the X-ray spectrum of the surrounding diffuse synchrotron nebula.

## 6. References

- Aharonian, F.A. and Akerlof, C.W., 1997, *Annual. Rev. Nucl. Part. Sci.*, 47, 273  
 Aharonian, F.A. et al., 1997, *A&A*, 327, L5  
 Atoyan, A.M. and Aharonian, F.A., 1996, *MNRAS*, 278, 525  
 Arons, J., 1996, *Space Sci. Rev.*, 75, 235  
 Bartlett, L.M., 1994, Ph.D. thesis, University of Maryland  
 Bogovalov, S.V. and Kotov, Yu.D., 1993, *MNRAS*, 262, 75  
 Borione, A. et al., 1997, *ApJ*, 481, 313  
 Bloom, E.D., 1996, *Space Sci. Rev.*, 75, 109  
 Cheung, W.M. and Cheng, K.S., 1994, *ApJ (Suppl)*, 90, 827  
 Davidson, K. and Fesen, R.A., 1985, *Ann. Rev. Astron. Astrophys.*, 23, 119  
 de Jager, O.C. and Harding, A.K., 1992, *ApJ*, 396, 161  
 de Jager, O.C. et al., 1996, *ApJ*, 457, 253  
 Elvis, M., 1997, to appear in ‘The Hot Universe’, IAU Symposium 188.  
 Fegan, D.J., 1997, *J.Phys. G: Nucl. Part. Phys.*, 23, 1013  
 Fierro, J.M., 1996, Ph.D. thesis, Stanford University.  
 Gould, R. J., 1965, *Phys.Rev. Lett.*, 15, 577  
 Hester, J.J. et al., 1995, *ApJ*, 448, 240  
 Jung, G.V., 1989, *ApJ*, 338, 972  
 Kennel, C.F. and Coroniti, F.V., 1984, *ApJ*, 283, 694  
 Marsden, P.L. et al., 1984, *ApJ*, 278, L29  
 Mohanty, G. et al., 1998, *Astroparticle Physics*, in press  
 Nolan, P.L. et al., *ApJ*, 409, 710  
 Rees, M. J. and Gun, J.E., 1974, *MNRAS*, 167, 1  
 Stepanian, A.A., 1995, *Nucl. Phys. B*, 39A, 207  
 Tanimori, T. et al. 1998, *ApJ*, 429, L33  
 van der Meulen, R.D. et al., 1998, *A&A*, in press  
 Weekes, T.C. et al., 1989, *ApJ*, 342, 379  
 Winkler, C., 1996, *A&A (Suppl.)*, 120, 637